J-PARC RADEN における
パルス中性子位相イメージングの開発

JAEA
関 義親

Talbot-Lau 干渉計の原理

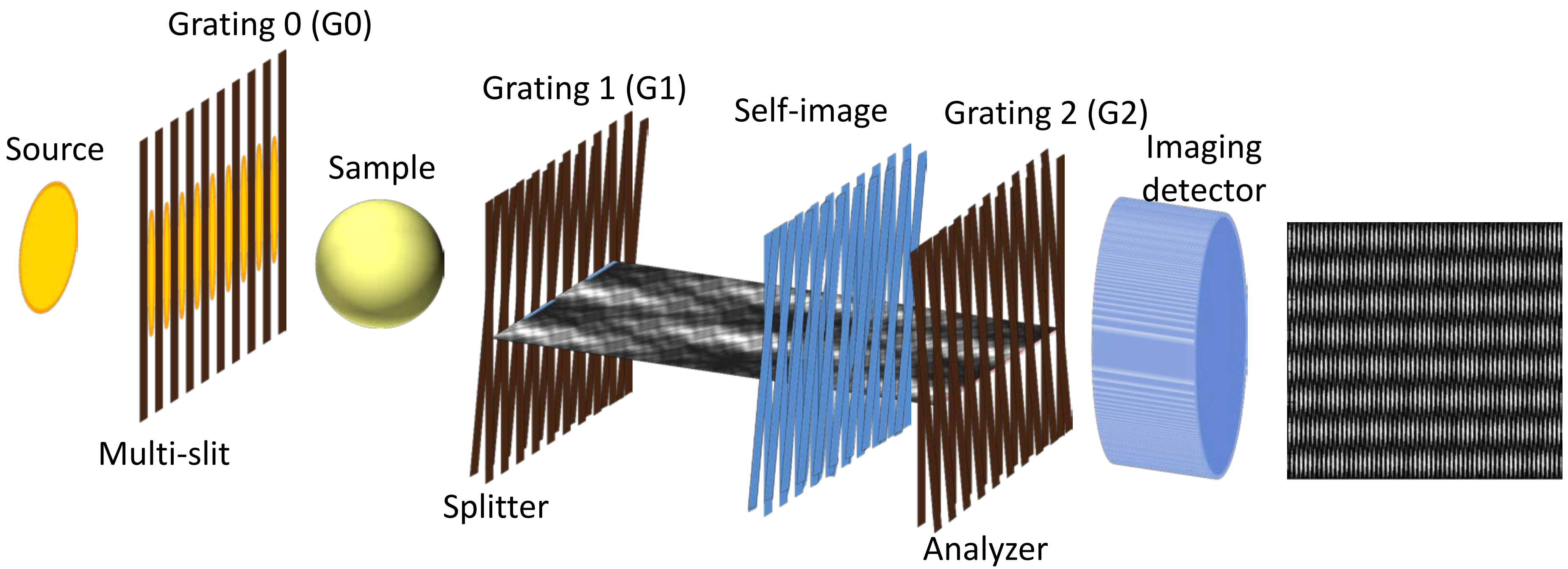

Fresnel回折場→ G2位置にG1直後と同じ強度分布：自己像
試料による自己像の歪みをG2とのモアレ縞で検出

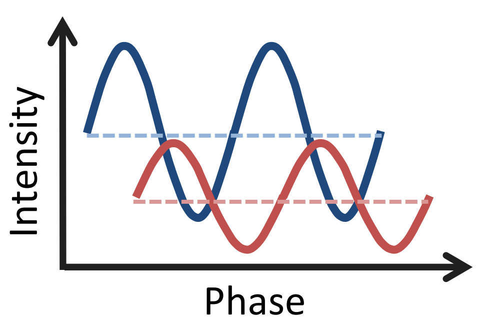

- 吸収コントラスト像（吸収断面積）
- 微分位相コントラスト像（散乱長）
- ビジビリティコントラスト像（小角散乱）

測定される物理量

微分位相イメージング

Phase of moiré fringe $\varphi(x,y) \propto \lambda^2 \frac{\partial}{\partial x} \int b(x,y)\rho(x,y)\,dz$

ビジビリティイメージング

Damping factor of visibility $\eta \simeq \exp[-\sigma_\Phi{}^2(x,y)\{1-\gamma(x,y;-pd_1)\}]$

Autocorrelation function $\gamma(x,y;\Delta x) \simeq \exp\left[-\left\{\frac{|\Delta x|}{\xi(x,y)}\right\}^{2H}\right]$

[b: Scattering length, ρ: Atomic density,
$\sigma_\Phi{}^2$: Standard deviation of phase, ξ: Correlation length, H: Hurst parameter]

Neutron beam

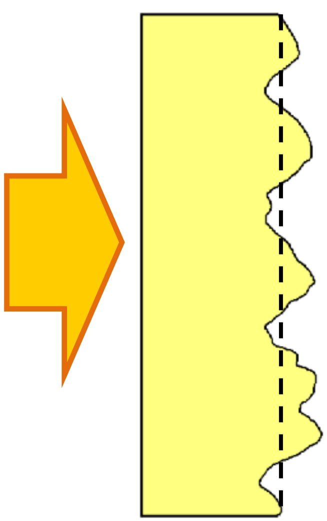

$$\Phi(x,y) = \underline{\Phi_s(x,y)} + \underline{\Phi_f(x,y)}$$

Phase shift due to averaged structure

Phase shift due to microstructures

J-PARC RADEN におけるTalbot-Lau 干渉法の高度化

- パルスビームでのTOF測定による
  波長分解型Talbot-Lau干渉法
  - 広波長域利用･高波長分解能の両立 → 高精度位相測定
  - 波長依存性を活かした解析
- 偏極中性子利用による
  磁気有感型Talbot-Lau干渉法
  - 磁場勾配測定
  - 磁場構造

格子のアライメント条件

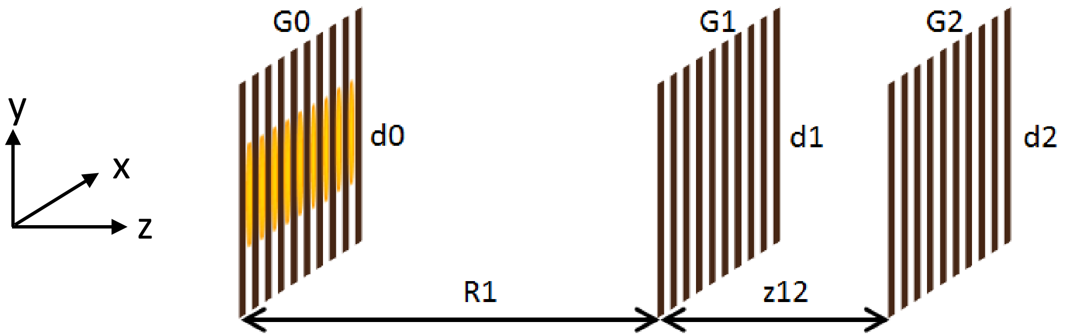

d_0, d_1, d_2: Grating pitches
R_1: Distance G0-G1
Z_{12}: Distance G1-G2
λ: Wavelength
p: Talbot order

- Talbot condition:
  Put G2 on the self-image position.

$$z_{12} = p\frac{{d_1}^2}{\lambda}M$$

p = 1 (G1: Absorption grating)
1/2 (G1: π/2 phase grating)
1/8 (G1: π phase grating)

- Lau condition:
  Superpose self-images from each line source of G0 constructively.

$$\frac{d_0}{d_2} = \frac{R_1}{z_{12}}$$

- Magnification due to spherical wave propagation

$$d_2 = d_1 M$$

$$M := \frac{R_1 + z_{12}}{R_1}$$

低ビームコヒーレンス下でのモアレ縞

Visibility of moiré fringe dependent on z_{12} (λ: fixed)

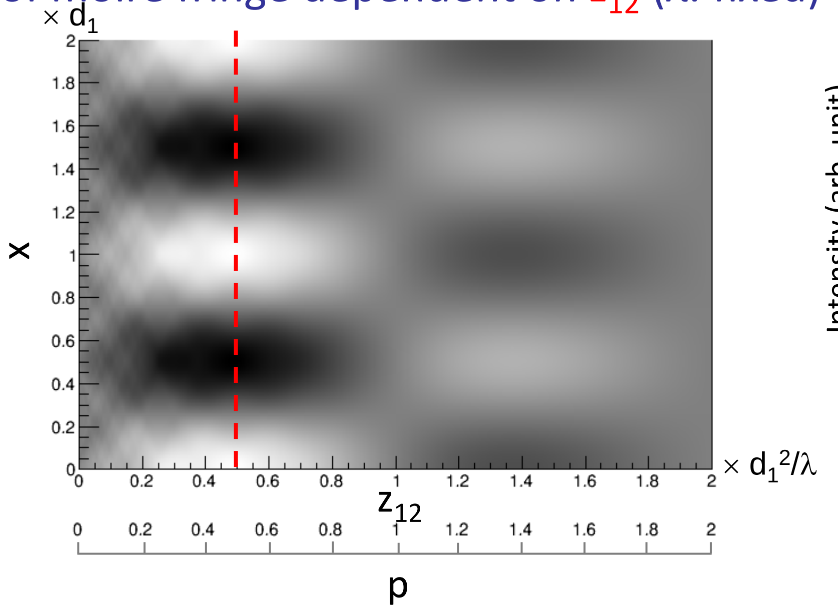

Moiré fringe between self-image of G1 and G2

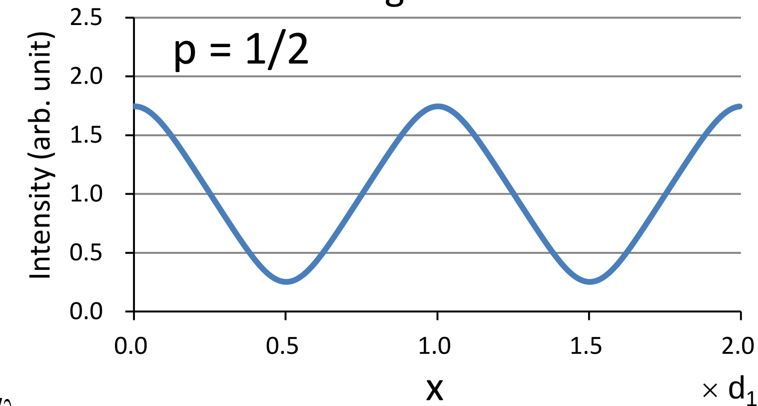

Moiré fringes are observable around $z_{12} = 0.5 \times d_{12}/\lambda$ (p = 1/2).

Visibility of moiré fringe dependent on λ (z_{12}: fixed)

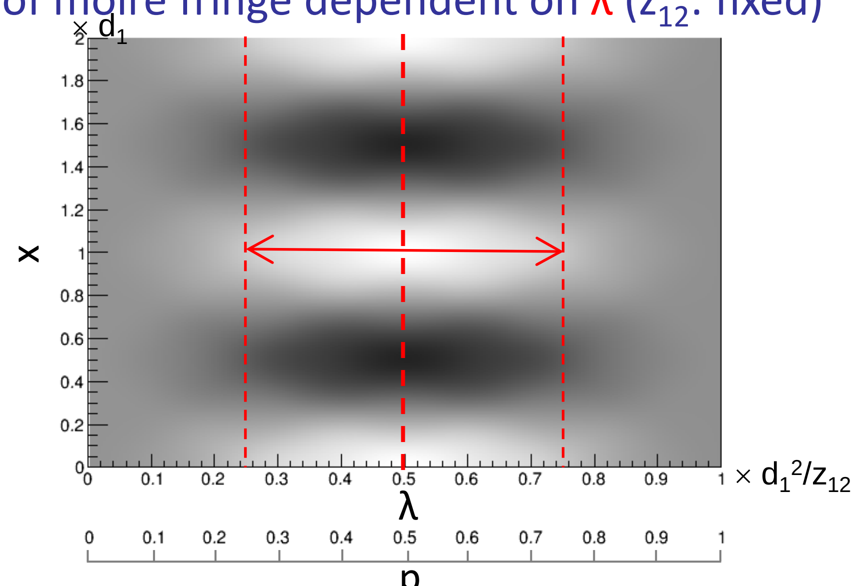

$$z_{12} = p\frac{{d_1}^2}{\lambda}$$

$$z_{12}\lambda \propto p$$

Moiré fringes are observable around $\lambda = 0.5 \times d_{12}/z_{12}$ (p = 1/2).

$\Delta\lambda/\lambda \sim 50\%$

Advantages of wavelength-resolved TL interferometry

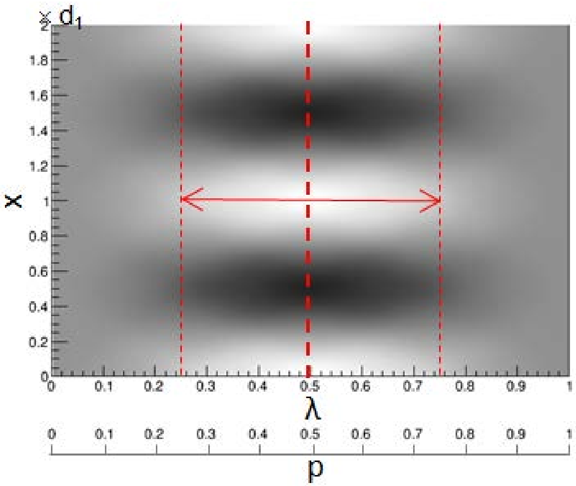

Phase determination precision for moiré fringe

$$\Delta\psi \propto \frac{1}{\sqrt{N}V}$$

Chromatic aberration of moiré phase

$$\Delta\psi_{\text{c.a.}}/_{\psi} = 2\Delta\lambda/_{\lambda}$$

N: Statistics
V: Moiré visibility
Δλ: Band width

- Wide wavelength band with fine wavelength resolution
  - Wide band → High statistics
  - Fine resolution → avoid chromatic aberration → High visibility

  → Increase phase precision and accuracy

- Wavelength dependence of physical quantity
  - Differential phase contrast imaging $\propto \lambda^2$
  - Visibility contrast imaging
    Autocorrelation function with different scales

Experiment at RADEN in J-PARC

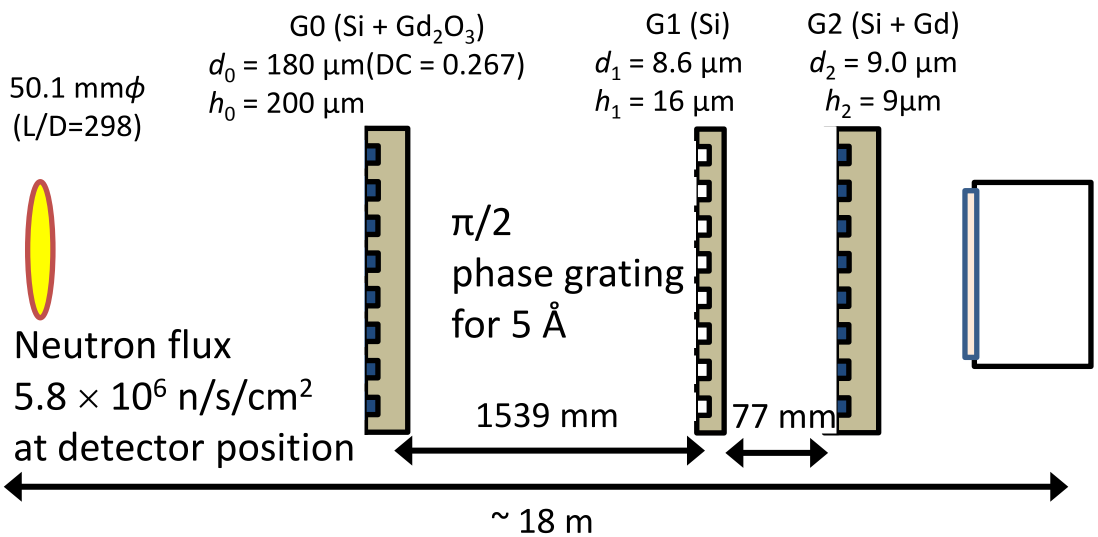

"μNID" detector

(Micro-pixel chamber + ^{3}He gas)

- D = 0.2 mm (512 × 512 pix)
- Δt = 0.5 ms
- $\Delta\lambda/\lambda$ = 4.5-1.3% (2.5 – 7.5 Å)
- Efficiency: 18%@25 meV

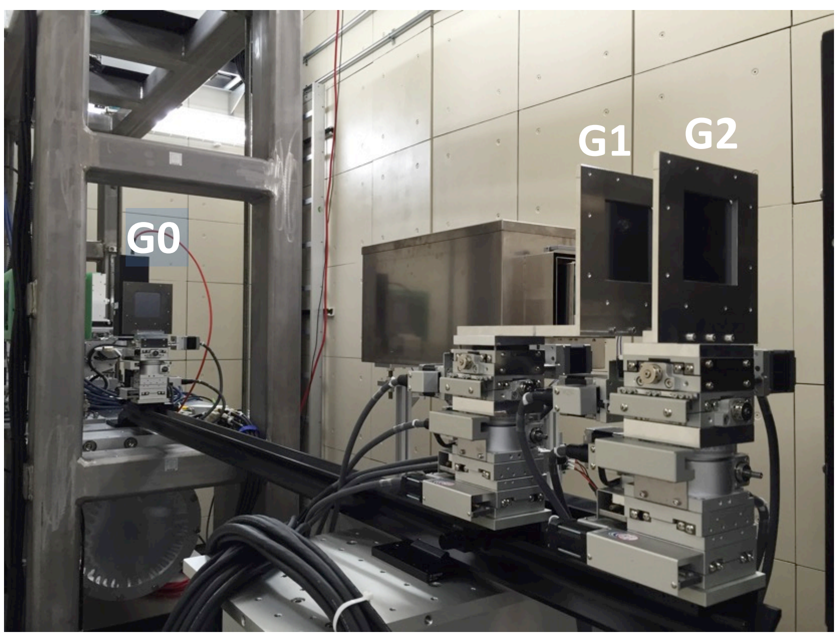

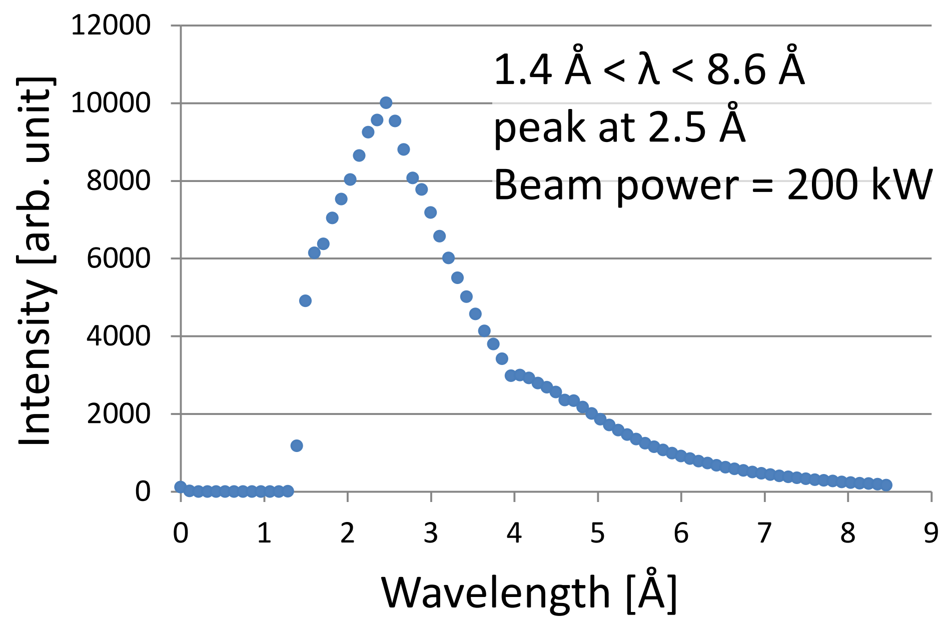

Fabrication of absorption grating with fine pitch (G2)

Gd evaporation method

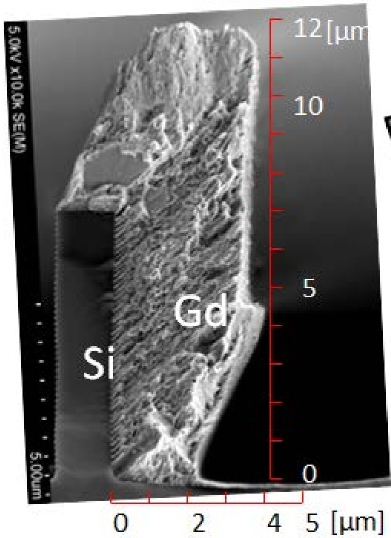

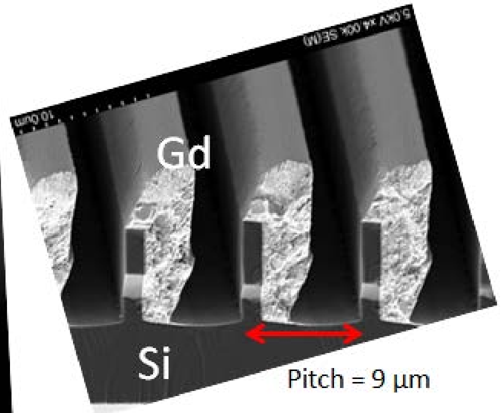

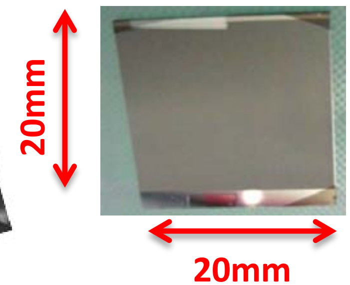

Neutron transmission image

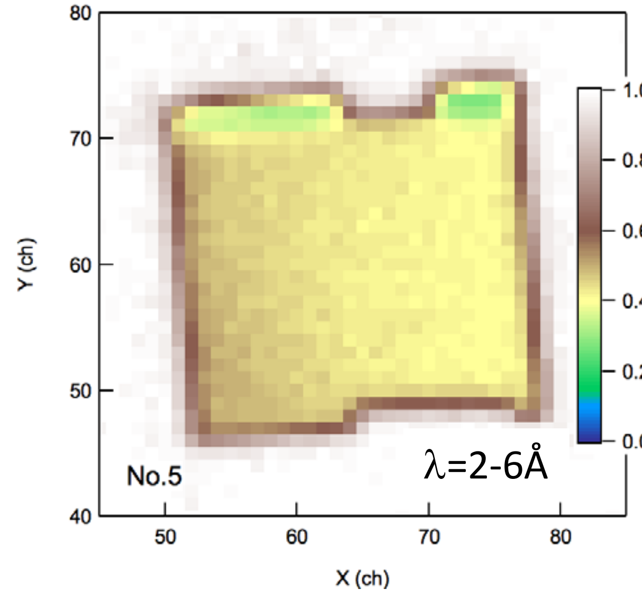

Wavelength dependence of neutron transmission

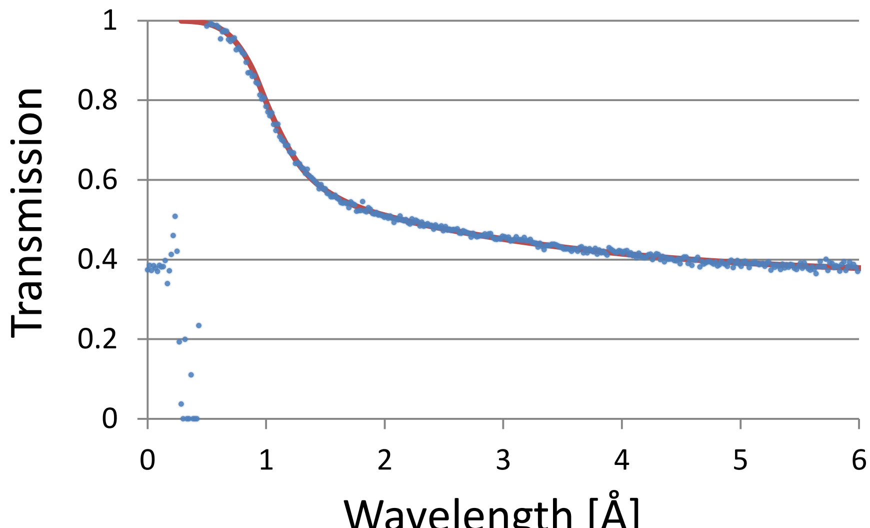

Effective Gd thickness 9.0 μm
Duty cycle 0.36

(On the assumption of ideal shape of Ronchi grating)

Fabrication of Absorption Grating

Gd based metallic glass imprinting

W. Yashiro et al., APEX, 7 (2014) 032501.
W. Yashiro et al., JJAP, 55 (2016) 048003.

ICP etching

Imprinting

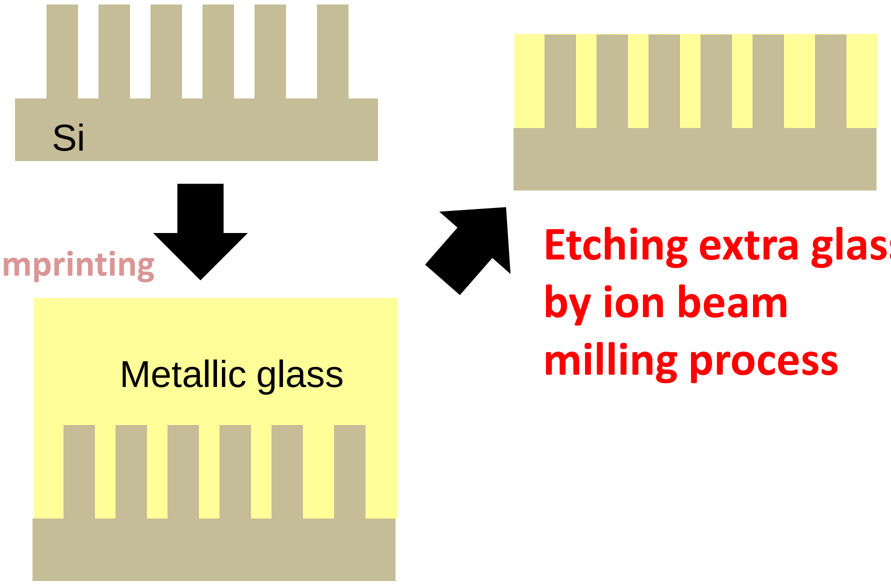

Etching extra glass by ion beam milling process

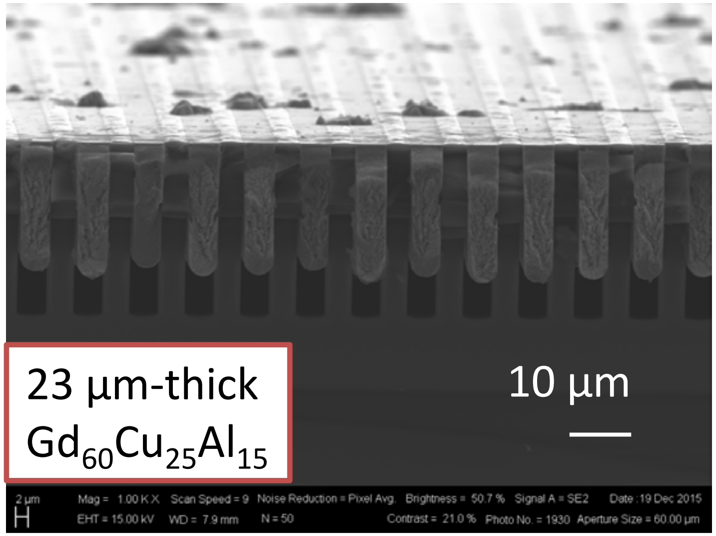

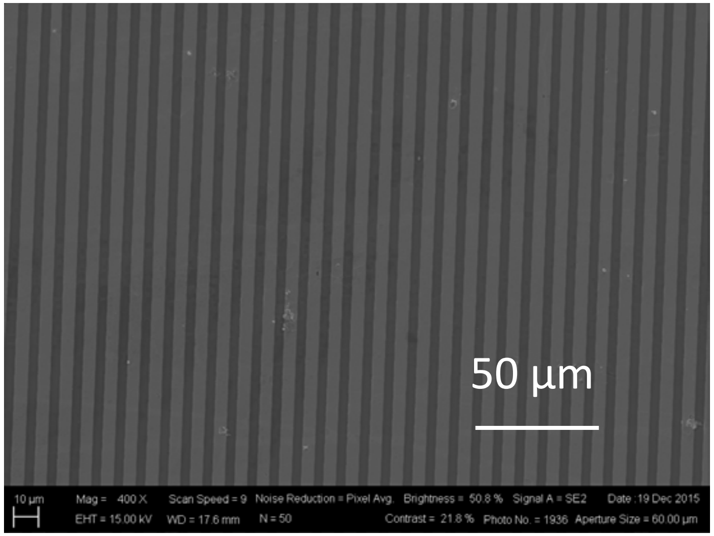

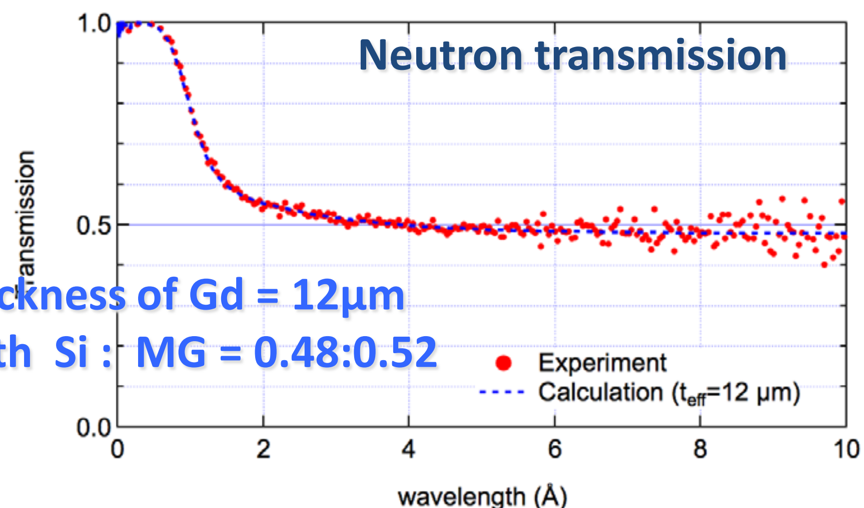

Effective thickness of Gd = 12µm
Grating width Si : MG = 0.48:0.52

Observation of moiré fringe (without sample)

Moiré fringe (at λ = 5.0 Å)

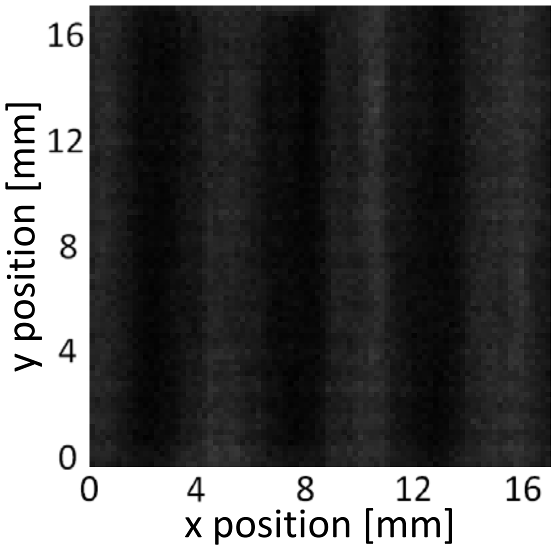

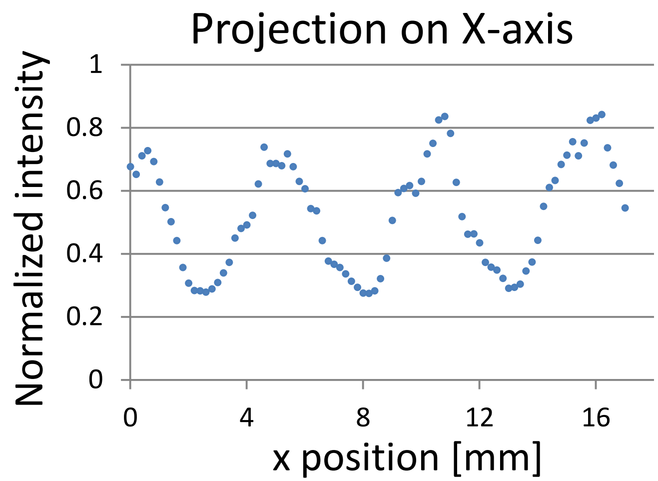

Fringe pattern can be seen over full wavelength range.

Wavelength dependence of moiré fringe (projected)

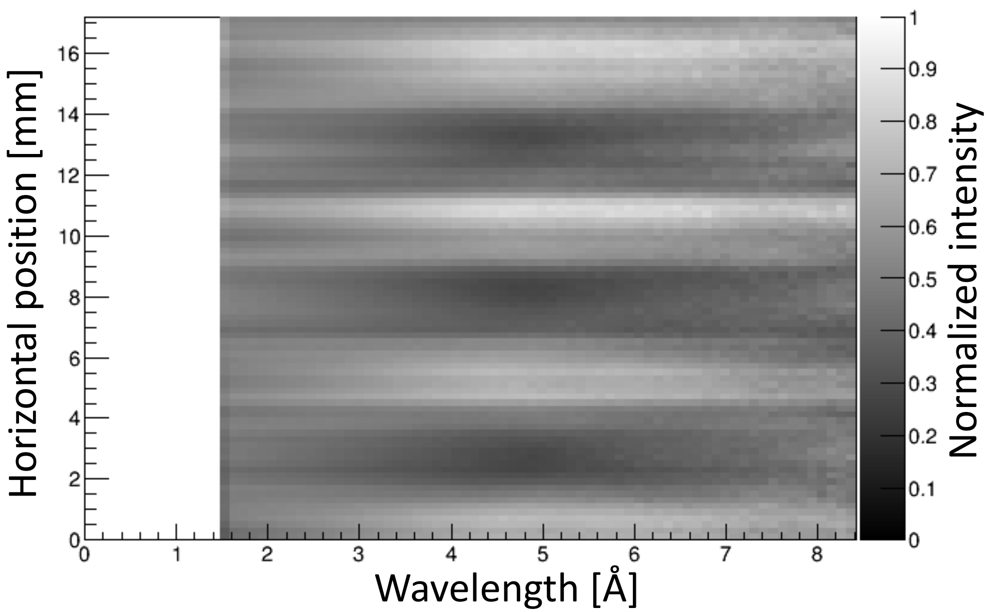

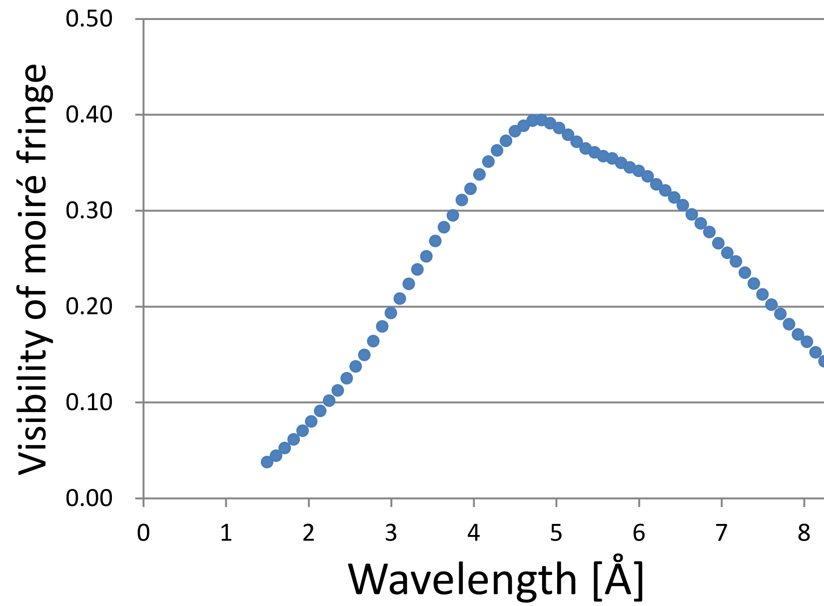

Phase imaging with TOF method

Ni, Ti, Al rods (ϕ=5mm)

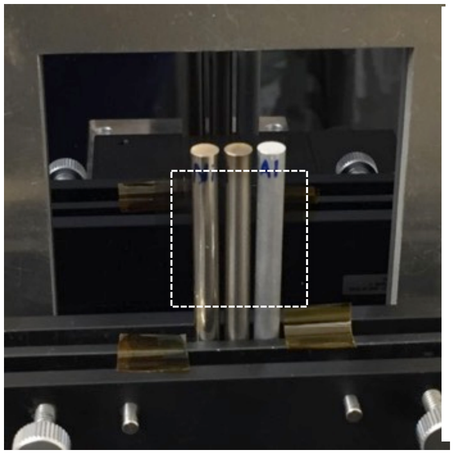

Absorption

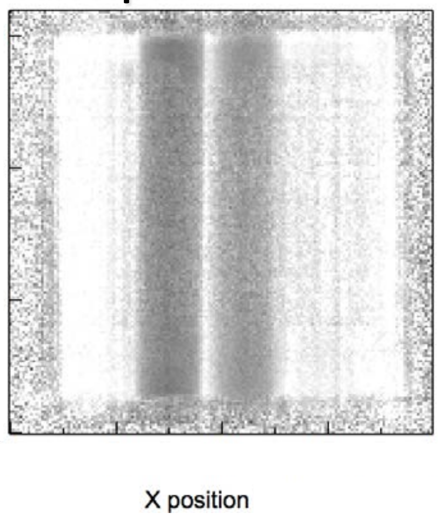

Differential Phase

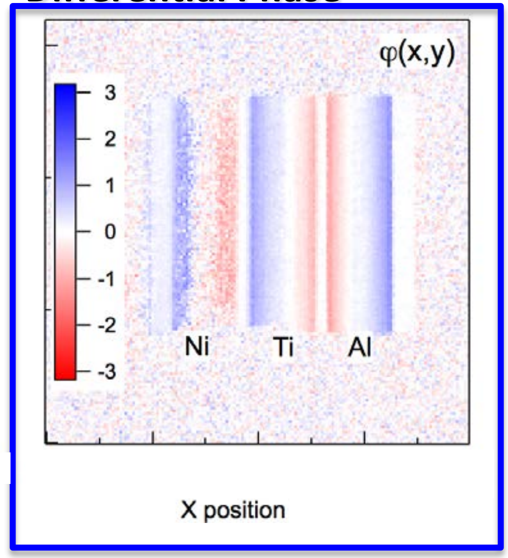

Visibility

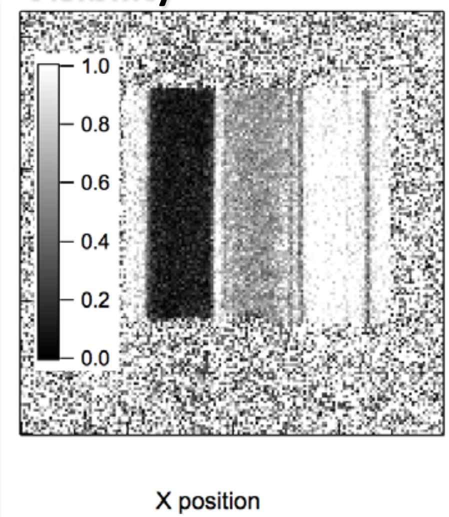

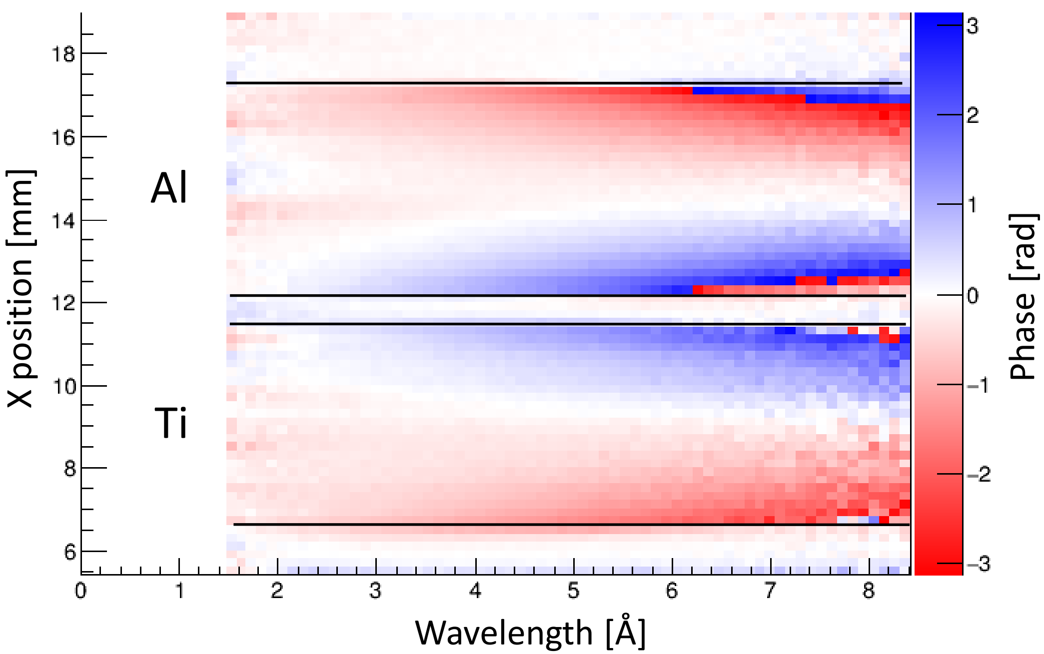

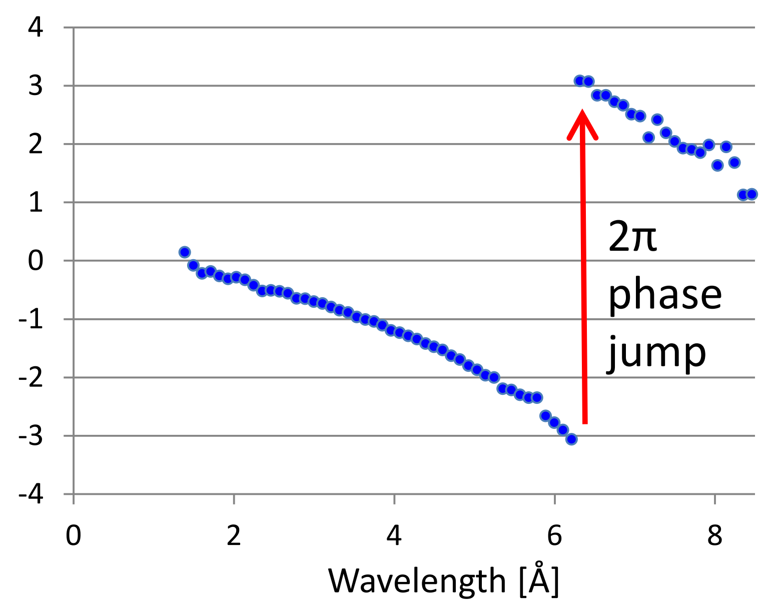

Wide wavelength band vs narrow wavelength band

λ = 5 Å (2.5-7.5 Å)
$\Delta\lambda/\lambda$ = 50%

High statistics,
but low contrast.

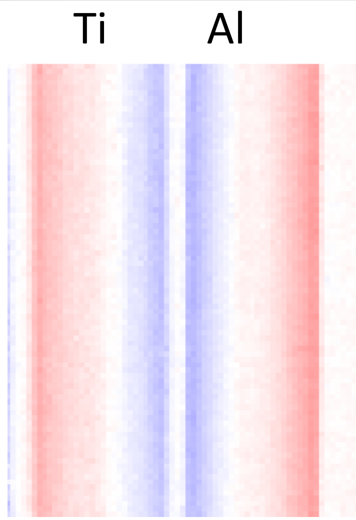

λ = 5 Å
$\Delta\lambda/\lambda$ = 2%

High contrast,
but noisy.

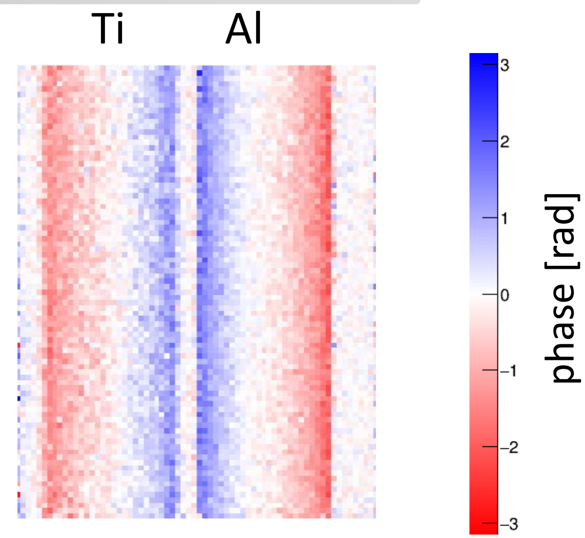

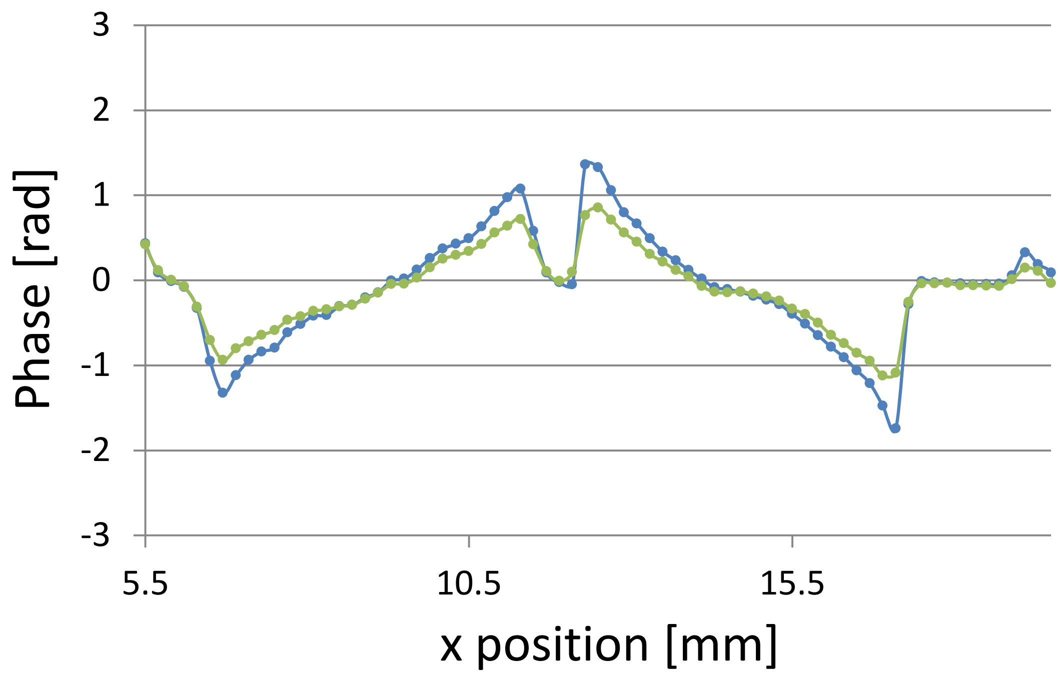

$\Delta\lambda/\lambda$ = 50%
Stat. error 4×10^{-3} rad

$\Delta\lambda/\lambda$ = 2%
Stat. error 3×10^{-2} rad

Wide wavelength band + TOF

Phase $\propto \lambda^2$

Phase unwrapping

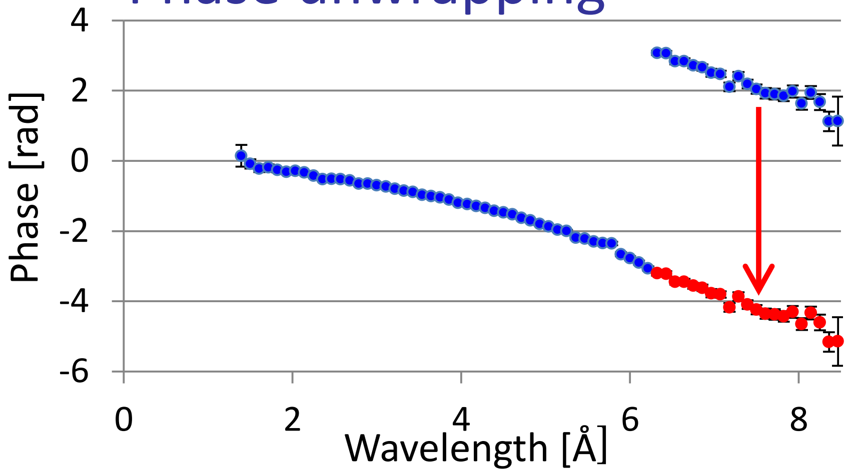

Fitting to parabola

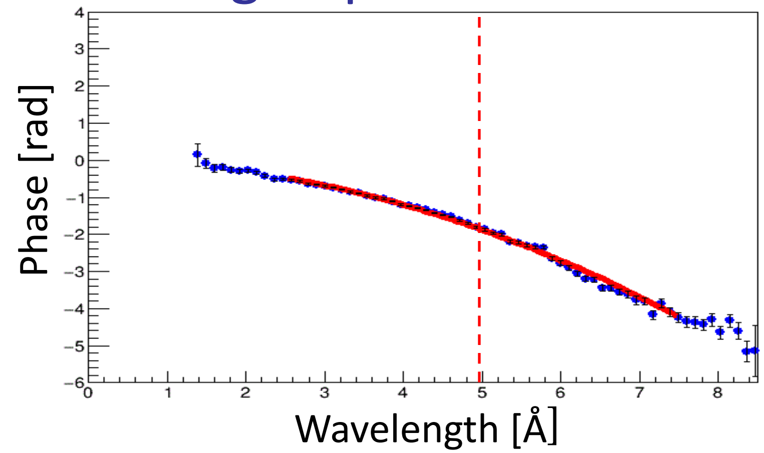

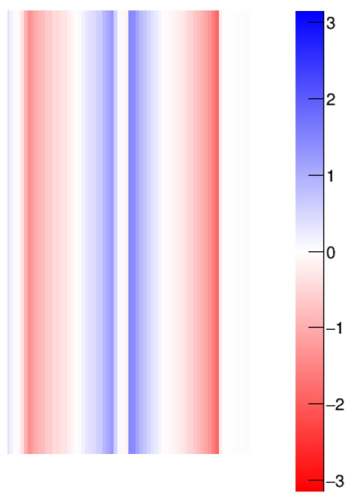

High statistics,
and high contrast.

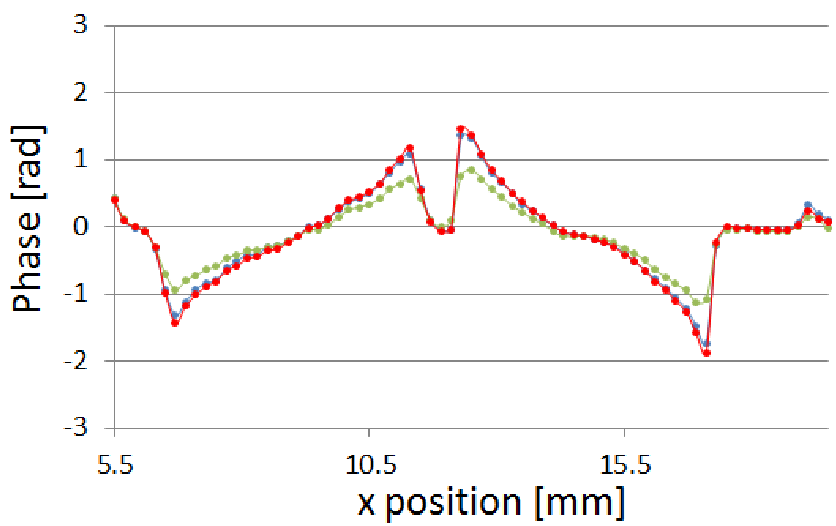

$\Delta\lambda/\lambda$ = 50%
Stat. error 4×10^{-3} rad

$\Delta\lambda/\lambda$ = 2%
Stat. error 3×10^{-2} rad

$\Delta\lambda/\lambda$ = 50% + TOF
Stat. error 4×10^{-3} rad

Summary

- Pulsed Talbot-Lau interferometry with TOF method at RADN, J-PARC.
- Differential phase contrast imaging with wide wavelength band (50%) and fine wavelength resolution (~ 3%).
- Phase analysis method with λ^2 dependence increases the dynamic range of phase detection in TL interferometer.
- Fabrication of absorption grating with Gd evaporation and imprinting of metallic glass
- Polarized TL interferometry